A Synoptic Case Study on Mean Structure of Mei-Yu in Taiwan

TAI-JEN GEORGE CHEN

Department of Atmospheric Sciences
National Taiwan University

(Manuscript received 5 March 1977, in revised form 14 March 1977)

ABSTRACT

A synoptic case study is carried out to reveal some characteristic features in the ending period of Mei-Yu season in Taiwan by the presentation of averaged fields of various meteorological elements during a period of six days from June 10 to 15, 1975. The consistency of the results in averaged fields including geopotential heights, winds, temperatures, humidities and cloud covers indicated the accuracy of initial data analysed. Mean vertical p-velocity ω computed kinematically were used as further check on the validity of the subjective analysis method employed. In general, vertical transport and twisting terms in the vorticity equation are one order of magnitude smaller than the other terms from a quasi-geostrophic consideration. Mean ω field in this study, on the other hand, suggested that they may not be neglected in middle and lower troposphere especially in the vicinity of the baroclinic zone and orographic areas. Results also indicated that the major moisture source in the area of interest was primarily from the Bay of Bengal. A thermal direct circulation with warm air rising and cold air sinking was shown across the baroclinic zone in the vicinity of Japan. Mean kinetic energy budget showed that the cross contour generation (8.32 Wm^{-2}), in connection with the thermal direct circulation, was dissipated in situ over the mean Mei-Yu area (-8.33 W m^{-2}). A value of -5.55 W m^{-2} due to the cross contour flow and a positive vaue of 4.11 W m^{-2} for residual term was obtained for the environment of the mean Mei-Yu area. Results clearly indicated that dominant processes were different within and outside the mean Mei-Yu area.

1. Introduction

Climatological data show that the annual rainfall distribution in the southeastern China possesses a relative maximum during the period of May and June. Continuous or intermittent precipitation is the characteristic feature in this rainy season. A similar phenomenon is found in central and eastern China and Japan with various time lags (e. g. Ramage 1971). It is called "Mei-Yu" or "Plum Rain" in China and "Baiu" in Japan.

Daily surface weather maps often indicate that a slow moving (or stationary) front runs from the vicinity of Japan southwestward into the southern China. This front is often termed as Mei-Yu front or Baiu front locally. Satellite pictures also reveal the nearly continuous cloud band along the front. A series of disturbances at different scales, ranging from hundreds to thousands kilometers, is frequently observed to propagate along this front northeastward.

Numerous works have been done on various aspects of Baiu front and its associated disturbances in the vicinity of Japan during the Baiu season over the last decade (e. g. Gambo 1970a, b, Matsumoto *et al.* 1970, 1971, Nitta *et al.* 1974). On the other hand, a relatively small amount of works is accomplished on the similar phenomena in the southeastern China. Much work remains to be done on the structures and dynamics of the weather systems during Mei-Yu season in southeastern China in addition to the traditional climatological studies. Thus, a case study was carried out to better understand the mean

structure of circulation systems during the ending period of Mei-Yu season in Taiwan. Observational data were analyzed to show the detailed distribution of horizontal winds, moisture and vertical motions. In addition, a kinetic energy (KE) budget study was made to reveal the role of different processes in the area during the period of interest.

2. Cases and Data

Cases have been chosen over the southeastern China and its vicinity including Mongolia, Korea, Japan, Indo-China and the southwestern North Pacific area. These areas have reasonably good coverage of surface and radiosonde observations except over the ocean. The area of interest is roughly bounded by 10°N and 55°N, 85°E and 150°E as shown in Fig. 1. There are a total of 140 radiosonde stations and 39 pibal stations within the region. Numerous surface and radiosonde data in the neighboring area were also used to help the analyses. These data were provided by the Chinese Central Weather Bureau on the coded form directly transmitted from Japan Meteorological Agency through a communication satellite.

Surface and mandatory level maps and NOAA-4 satellite pictures as received from Chinese Air Force Weather Central were used in the case selection during Mei-Yu season. These data were examined to see if there was a typical Mei-Yu front, i.e. the existence of a cloud band along a nearly stationary front, in the vicinity of Taiwan and the southern China. Also, the hourly rainfall observations over the surface stations in Taiwan were used to identify the characteristic feature of continuous to intermittent rains.

Cases of 6-day period from June 10 to June 15, 1975 appeared to be a rather well-defined Mei-Yu regime in Taiwan. In addition, the available data from both the surface and radiosonde observations were most complete during these time periods. Thus, this case was chosen for the present study. This hopefully will help to insure that the results be more representative.

Fig. 2 shows the 6-day rainfall totals in Taiwan from June 10 to June 15, 1975. Moderate to heavy rains were generally observed to the west of the Central Mountain Range during this period. Thus, some limited areas along the west coast received a total of more than 300 mm within 6 days. On the other hand, light to no rain was usually the case to the east. Therefore, a total of less than 20 mm rainfall was

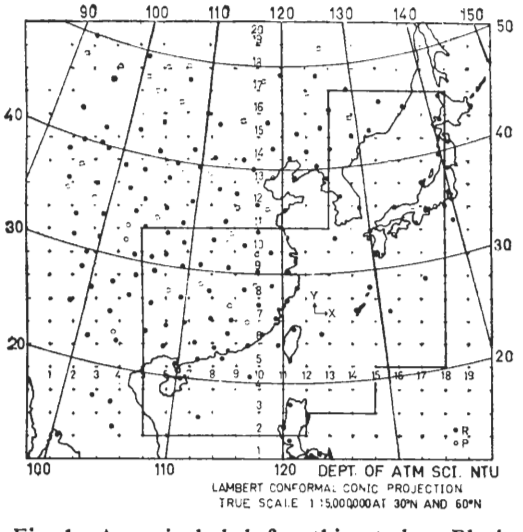

Fig. 1. Area included for this study. Black dots and circles show radiosonde and pibal stations, respectively. Plus signs indicate the grid arrays. Inner solid lines are the boundaries of the mean Mei-Yu area.

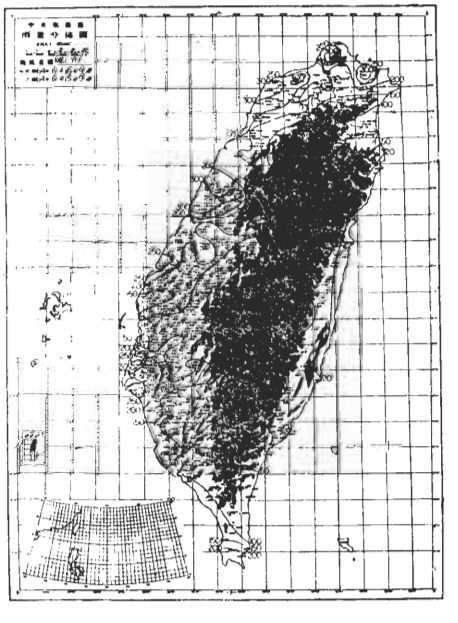

Fig. 2. Total rainfalls (in mm) during the periods of June 10, 0900 LST to June 15, 0900 LST, 1975.

found along the east coast.

3. Procedures

A computational domain consists of 20 by 19 grids with a grid spacing of 240 km valid at 30°N and 60°N on a Lambert projection map (see Fig. 1). Data were subjectively analyzed on isobaric surfaces at mandatory levels with the aid of numerous vertical cross sections. Geopotential heights, temperatures, dew points, wind speeds and wind directions were then interpolated at the grid points. Data at other pressure levels were obtained by linear interpolation with respect to pressure when needed.

As mentioned previously that, the data used in this study were interpolated from a subjective analysis. A two-dimensional filter is, therefore, necessary to eliminate short-wavelength components contained. The smoothing scheme (25 points) applied is identical to that in Chen (1976). Thus, the gradients and absolute magnitude of the various scalar parameters in the final analyses were well preserved while the short-wave noises were successfully eliminated.

Kinematic ω's were computed using O'Brien's (1970) adjustment scheme. The vertical velocities specified at the upper boundary (100 mb) were obtained by the adiabatic method (Chen 1976). At the lower boundary, the frictional induced ω's were computed using a parameterization scheme identical to that of Holton (1972). The orographic induced vertical motions were computed along the smoothed terrain using the observed winds at 850 mb and 700 mb for surface elevations below 1500 m and above 3000 m, respectively. While the surface elevations of 1500–3000 m, the averaged winds of 850 mb and 700 mb were used for computations. Smoothed surface elevations adopted are identical to those used in Tsay (1975). The ω's at lower boundary thus computed were then assumed at 850 mb level. This choice proved to be most successful in producing the acceptable boundary ω's in view of satellite pictures and synoptic experience.

The kinetic energy budget equation can be written as follows:

$$\frac{\partial K}{\partial t} = -\frac{1}{gA}\int_A\int_{P_2}^{P_1}\nabla\cdot(k\mathbf{V})dPdA \qquad (1a)$$

$$-\frac{1}{gA}\int_A\int_{P_2}^{P_1}\frac{\partial k\omega}{\partial P}dPdA \qquad (1b)$$

$$-\frac{1}{gA}\int_A\int_{P_2}^{P_1}\mathbf{V}\cdot\nabla\Phi dPdA \qquad (1c)$$

$$+R \qquad (1d)$$

where

$$K=\frac{1}{gA}\int_A\int_{P_2}^{P_1}kdPdA \qquad (2)$$

$$k=\frac{1}{2}(u^2+v^2) \qquad (3)$$

$$\Phi=gz \qquad (4)$$

and A is area, $p_2(p_1)$ is the pressure at higher (lower) level. Other notations are conventional.

Terms (1a) and (1b) are boundary flux terms through the horizontal and vertical walls, respectively. Term (1c) is the generation term due to cross contour flow. Term (1d) is residual term taken as the difference between local accumulation on the left hand side and the summation of terms directly computed on the right hand side.

A simple centered finite-difference scheme was used to compute all spatial derivatives. Notice that the terms on the right hand side of equation (1) were instantaneous values, while the local accumulation was averaged value at a fixed time taken as the difference between 12 h after and 12 h before. The KE budget terms was then averaged for all the time periods after integration. All the parameters observed and computed were also averaged during a 6-day time period to show the mean structure of the circulation systems in Mei-Yu season.

4. Results

(I) Mean Circulation Patterns

A low center was found along the boundary of mainland China and Indo-China at 1000 mb. The trough ran from Honshu southwestward, passing through Bashi Channel, and extended into this low center. Another trough was also discernible over the central and northern China. A high center was located in the vicinity of the Sea of Okhotsk. Ridge line extended from this center passing through Hokkaido and Korea into east coast of China(Fig. 3). The observed wind fields (not shown) were found essentially in a rather good qualitative agreement with those could be expected from the contour analyses. In the vicinity of Taiwan, the cold air in the surface layer originally coming from the vicinity of the Sea of Okhotsk and the warm

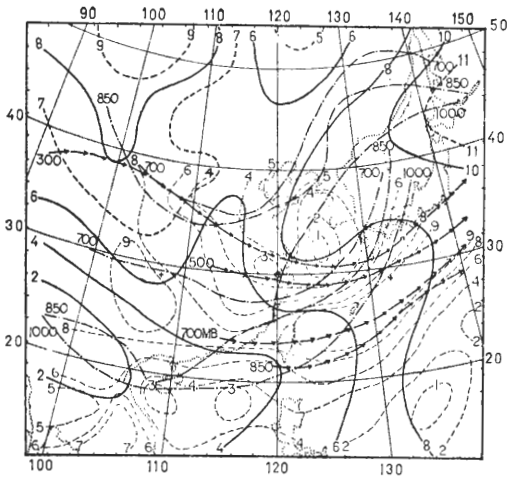

Fig. 3. Geopotential heights (solid or dashed) in dam at 1000 mb. Thin dashed lines show NOAA-4 mean cloudiness. Dash-dot lines are shear lines at indicated levels. Arrows indicate the positions of jet stream at different levels.

air from the south apparently converged along the trough line.

The height contours and grid point resultant winds at 850 mb and 700 mb were presented on Fig. 4 and Fig. 5, respectively. Notice that the wind shear lines were coincident with the troughs and ridges at both levels. Also, the observed winds were in a considerably good agreement with the analyzed contours from a gradient

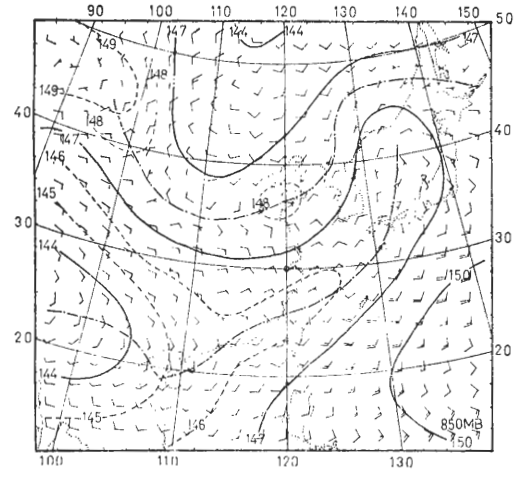

Fig. 4. Geopotential heights (solid or dashed) in dam and resultant wind vectors at grids on 850 mb. Dash-dot lines indicate ridges and troughs (i.e. shear lines).

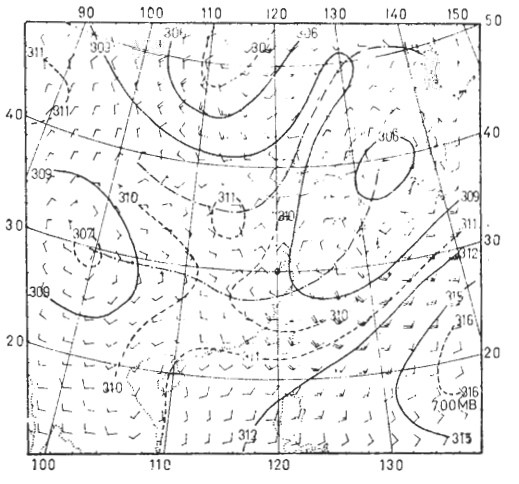

Fig. 5. Same as Fig. 4, except at 700 mb.

wind consideration. While a rather weak low center was discernible on 850 mb in the Sea of Japan, a well-defined one on 700 mb could be found in the same area. On 850 mb, a trough line extended from this center southwestward passing through the area to the north of Taiwan into the low center located in the southern China. The slope of this trough is estimated to be about 1:165 from 1000 mb to 850 mb in the vicinity of Taiwan. An additional northward shift of this trough was found at 700 mb with the averaged slope of 1:150 from the 850 mb level in the same area.

The low center in the southwestern China at 700 mb was found to have a northward tilt from that of 850 mb. An anticyclone center, although weak, was discernible in northern China at both levels. Thus, to the north of the trough the easterly to northerly winds were common while to the south of it the southwesterlies were predominant, especially in the vicinity of Taiwan. While the southwesterly jet on 850 mb was located in Bashi Channel, the jet on 700 mb was found across the central Taiwan (see Fig. 3, 4, 5).

The main trough at 500 mb extended southwestward from the well-developed low center over the Sea of Japan to the northeast of Taiwan (Fig. 6). The mid-latitude trough was located over Mongolia with a very small tilt from its location on 700 and 850 mb. An anticyclone center was found in the South China Sea. Thus, the northwesterlies prevailed at this level in the vicinity of Taiwan. Well defined

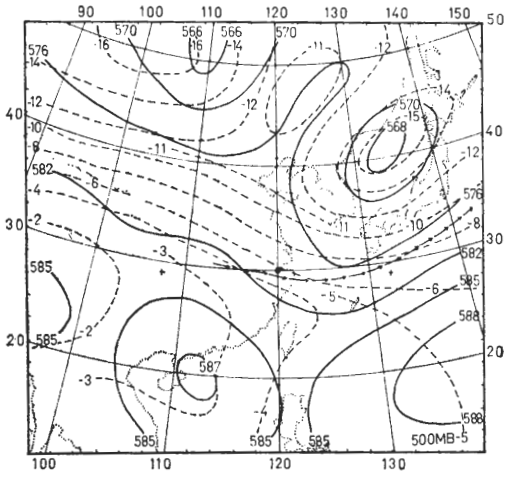

Fig. 6. Geopotential heights (solid) in dam and isotherms (dashed) in °C on 500 mb. Arrows indicate the jet stream.

baroclinic zone was situated to the north of 30°N and the jet was found to the warm side of it. The typical patterns of cold low (or trough) and warm high (or ridge) are also clearly shown at this level.

Circulation patterns on 300 mb (Fig. 7) were quite similar to those on the 500 mb. Weak winds were observed within the high and low centers and along the ridge lines as would be expected. Northwesterly jet was found in the northwestern China while the southwesterly jet extended from the southeast of Japan to eastern China. In general, the observed winds were in a good agreement with the contour lines in view of the geostrophic and gradient wind relationships.

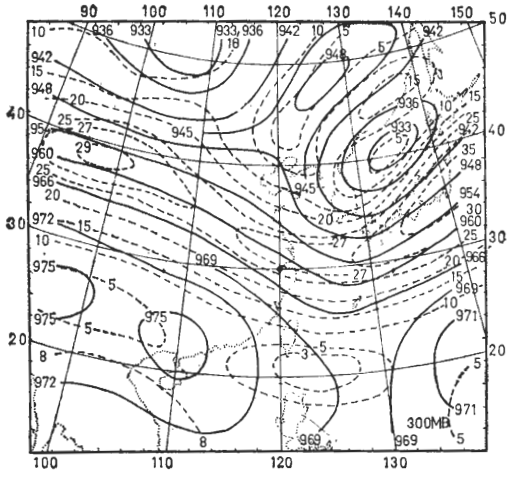

Fig. 7. Geopotential heights (solid) in dam and isotachs (dashed) in m s^{-1} at 300 mb.

(II) Mean Vertical Motion Field

In general, the upward motions prevailed to the south and east of the troughs while the downward motions predominated behind the troughs and to the east and south of the ridges at all levels from 850 mb to 500 mb (Fig. 8, 9, 10). In other words, ridge and trough lines (or shear lines) approximately separated upward motions from downward motions in most area. Recall that the ω's due to the boundary friction and terrain induced components obtained at 850 mb were taken as the lower boundary.

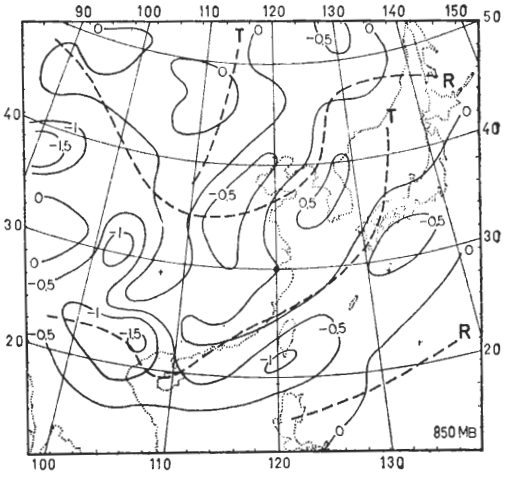

Fig. 8. Mean ω's in μb s^{-1} on 850 mb. Dashed lines show ridge (R) and trough (T) lines.

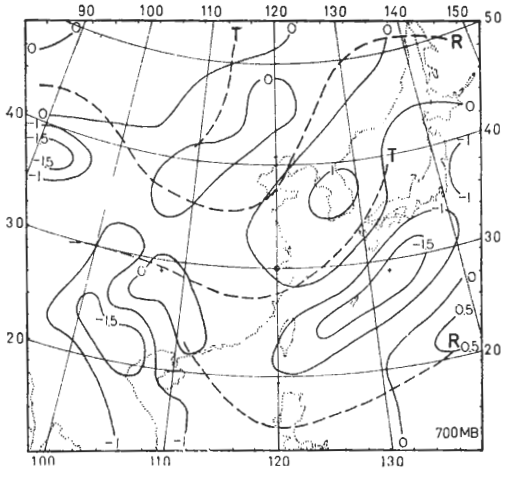

Fig. 9. Same as Fig. 8, except on 700 mb

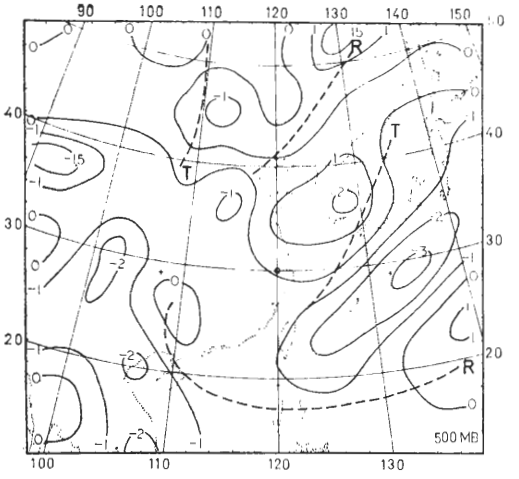

Fig. 10. Same as Fig. 8, except on 500 mb.

Thus, the upward motions in the southwestern China were primarily due to these two effects. Overall, the computed kinematic ω's are synoptically reasonable on both the patterns and magnitudes.

Maximum centers of upward motion were located to the south of Japan extending southwestward into the vicinity of Taiwan with the values of $-0.5\ \mu b\ s^{-1}$, $-1.5\ \mu b\ s^{-1}$ and $-3.0\ \mu b\ s^{-1}$ on 850 mb, 700 mb and 500 mb, respectively. Maximum downward motions were found over Korea with the corresponding values of $0.5\ \mu b\ s^{-1}$, $1.0\ \mu b\ s^{-1}$ and $2.0\ \mu b\ s^{-1}$.

(III) Mean Moisture Field

The maximum gradient of mixing ratio was found over the East China Sea on both 850 mb and 700 mb (Fig. 11, 12). Thus, the moist air was confined in the southeastern China with the dry air located to the north over the eastern China and the Yellow Sea. The moist tongue situated over the southestern China and Indo-China was apparently carried in from the Bay of Bengal by the low level southwesterlies (see also Fig. 4, 5). Moisture flux into the vicinity of Taiwan from the South China Sea is also clearly indicated. The mean cloudiness as computed from the NOAA-4 satellite pictures was found to be reasonably well correlated with the mean relative humidity on 700 mb (Fig. 13). Also, the maximum mean cloudiness

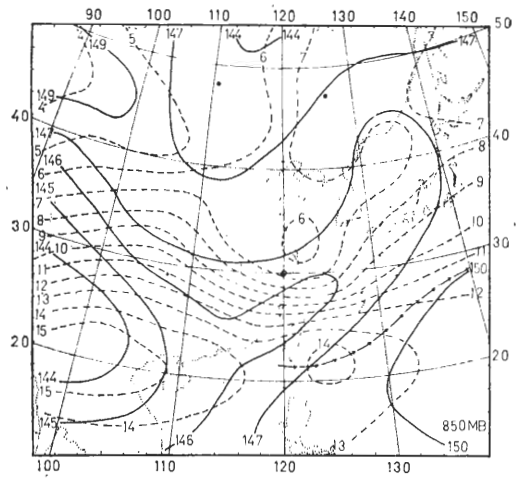

Fig. 11. Mixing ratio (dashed) in g Kg^{-1} and geopotential height (solid) in dam on 850 mb. Arrows show the jet stream.

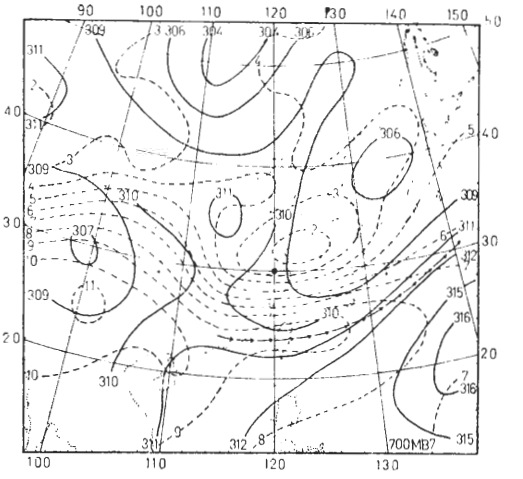

Fig. 12. Same as Fig. 11, except on 700 mb.

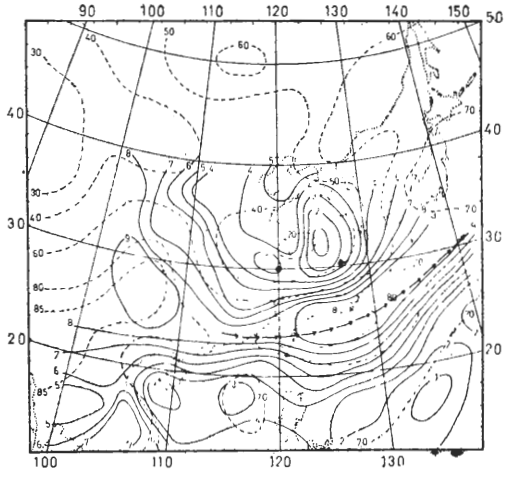

Fig. 13. Mean relative humidity (in %) on 700 mb (dashed) and mean cloudiness (in tenth) of NOAA-4 (solid). Arrows show the jet stream on 700 mb.

Table 1. The mean kinetic energy budget terms over the 19×20 grid area averaged during the period of June 10, 1200Z (T2) to 15,0000Z (T11), 1975. Symbols are: LK- local accumulation; HK- horizontal flux; CK- cross contour term; RK- residual term. Units are Wm^{-2}.

MB	LK	HK	VK	CK	RK
150-100	−.14	−.10	.65	.09	−.78
200-150	−.16	.04	.52	.10	−.82
250-200	−.09	.07	.10	.41	−.67
300-250	−.07	.06	−.27	.44	−.30
350-300	−.07	−.00	−.37	.21	.10
400-350	−.05	−.01	−.29	.19	.05
450-400	−.04	−.01	−.14	.18	−.06
500-450	−.04	−.02	−.08	.14	−.08
550-500	−.04	−.02	−.07	.11	−.05
600-550	−.03	−.01	−.06	.09	−.05
650-600	−.02	−.01	−.03	.10	−.08
700-650	−.01	.00	−.02	.12	−.11
750-700	−.01	.01	−.03	.15	−.14
800-750	−.01	.01	−.02	.18	−.18
850-800	−.01	.01	−.01	.24	−.24
300-100	−.46	.06	1.00	1.04	−2.57
500-300	−.21	−.04	−.89	.72	.00
850-500	−.12	−.01	−.25	1.00	−.86
Total	−.79	.00	−.14	2.76	−3.42

was found along the jet stream on 700 mb and trough line on 1000 mb (Fig. 3, 13).

(IV) Mean Kinetic Energy Budgets

The mean Mei-Yu area (MMY) in this study is defined as the area bounded by the ridge lines on 850 mb in the vicinity of the Mei-Yu front (Fig. 1). The mean kinetic energy budget (MKE) over the whole area of 19×20 grids and over the MMY area are shown in Tables 1 and 2 and Figs. 14 and 15(a). The cross contour flow was the dominant process in generating KE with a total contribution of 2.76 $W m^{-2}$ over the whole area and a value of 8.32 $W m^{-2}$ over the MMY area. The local accumulation term indicated the local decrease of KE at all levels during these 6-day periods

Table 2. Same as Table 1, except over the mean Mei-Yu area (MMY).

MB	LK	HK	VK	CK	RK
150-100	−.13	.00	.87	.68	−1.69
200-150	−.14	.12	.65	.91	−1.82
250-200	−.05	−.02	.12	1.52	−1.67
300-250	−.03	−.01	−.36	1.60	−1.26
350-300	−.04	−.08	−.49	.98	−.46
400-350	−.05	−.08	−.35	.64	−.25
450-400	−.05	−.09	−.17	.41	−.20
500-450	−.04	−.10	−.10	.26	−.10
550-500	−.03	−.08	−.10	.19	−.05
600-550	−.03	−.05	−.08	.19	−.08
650-600	−.02	−.03	−.05	.19	−.13
700-650	−.01	−.01	−.04	.20	−.16
750-700	−.01	.00	−.05	.20	−.15
800-750	−.01	.01	−.05	.18	−.15
850-800	−.01	.01	−.03	.18	−.17
300-100	−.35	.09	1.28	4.71	−6.44
500-300	−.18	−.35	−1.10	2.29	−1.02
850-500	−.11	−.15	−.40	1.32	−.88
Total	−.64	−.40	−.22	8.32	−8.33

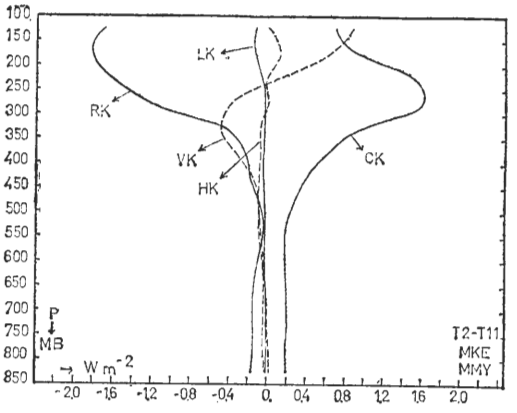

Fig. 14. Vertical profiles of mean KE budget (MKE) from June 10, 1200Z (T2) to June 15, 0000Z (T11), 1975 over the mean Mei-Yu area (MMY). Units are in Wm^{-2} and mb for the abscissa and ordinate, respectively. Abbreviations are as follows: LK-local accumulation; HK-horizontal flux; VK-vertical flux; CK-cross contour term; RK-residual term.

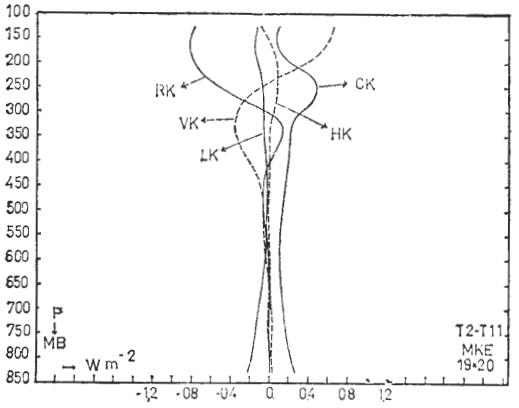

Fig. 15(a). Same as Fig. 14, except for the area of 19×20 grids.

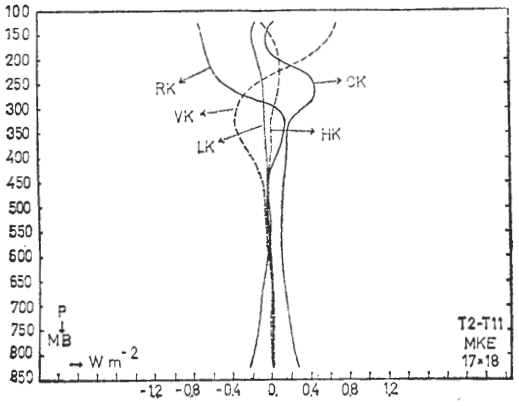

Fig. 15(b). Same as Fig. 14, except for the area of 17×18 grids.

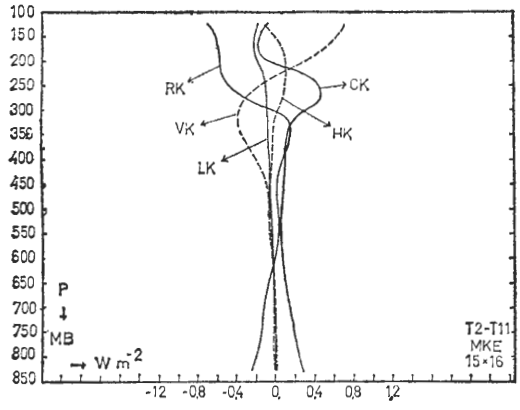

Fig. 15(c). Same as Fig. 14, except for the area of 15×16 grids.

with a value of -0.79 W m^{-2} and -0.64 W m^{-2} for the corresponding area.

The vertical transport of KE contributed insignificantly over the whole atmosphere. However, it was an important contributor in balancing the KE at each level with a net divergence of vertical flux below 250 mb. Thus, the increase of KE in the upper troposphere above that level due to vertical transport from the lower and middle troposphere has a value of 1.27 W m^{-2} and 1.64 W m^{-2} over the whole area and the MMY area, respectively. Horizontal flux term, although small at each level, showed a net total outward flux of -0.40 W m^{-2} from the MMY area. As a result, the frictional term taken as a residual showed dissipation of total KE of 3.42 W m^{-2} over the whole area and 8.33 W m^{-2} over the Mei-Yu area. Thus, the cross contour generation of KE (8.32 W m^{-2}) over the MMY area was totally dissipated in situ (-8.33 W m^{-2}) in the mean. Taking the differences between the values of Tables 1 and 2, a value of -5.55 W m^{-2} due to the cross contour flow and a value of 4.91 W m^{-2} for the residual term was obtained for the environment of MMY area. Vertical profiles of budget terms over the smaller area of 17×18 and 15×16 are also shown in Fig. 15(b), (c) for comparison. The very similar profiles to those over the 19×20 grids (Fig. 15(a)) in both shapes and magnitudes are clearly indicated.

5. Summary

A synoptic case study was carried out on a typical Mei-Yu situation in Taiwan during the period of June 10 to June 15, 1975. Rainfall distribution together with the synoptic analyses suggest that the weather systems were of major importance in causing local precipitation. This is at variance with the traditionally cited major cause of topographical effect under the low level southwesterlies. A well-defined wind shear line on 700 mb and 850 mb levels was found in the vicinity of the surface front. Results also indicated the major moisture source of the Bay of Bengal in the area of interest.

Mean ω field suggested that the neglect of twisting and vertical transport processes in the operational model might cause some errors in predicting the system's movement. Thermal direct circulations with warm air rising and cold air sinking was found, especially across the baroclinic zone in the vicinity of Japan (Fig. 6, 10). As a result, cross contour flow contributed to a generation of KE of 8.32

$W\,m^{-2}$ in the mean Mei-Yu area in comparison with a value of $2.76\,W\,m^{-2}$ over the whole area of 19×20 grids. A decrease of KE of $5.55\,W\,m^{-2}$ was then obtained for the environmental region of the MMY area due to the cross contour flow from lower to higher heights. Thus, a positive value of $4.91\,W\,m^{-2}$ through residual term was required over the same area for balancing the KE. Similar results of positive values in the residual term were also reported in other case studies for the surface anticyclone and upper ridge situations (e. g. Chen and Bosart 1977, Kung and Baker 1975). Notice that the cross contour generation of KE ($8.32\,W\,m^{-2}$) was almost completely dissipated ($-8.33\,W\,m^{-2}$) in situ over the MMY area in the mean.

In view of the characteristic features revealed in the present study of Mei-Yu, a diagnostic study of individual case on a daily basis is thus needed to better understand the dynamics of the circulation systems in the Mei-Yu regime. This has been done and will be presented on the other paper. The consistency of the results among averaged fields indicated the accuracy of initial data analyzed. This hopefully will insure that the results and conclusions of a diagnostic case study be more representative.

Acknowledgment: The research reported here represents a portion of the results in Mei-Yu Projects termed "Synoptic-Dynamic Study of Mei-Yu in Taiwan". Support was provided by National Science Council Grant NSC-65M-0202-01(03). The Chinese Central Weather Bureau and Chinese Air Force Weather Central provided most of the data used. Mr. Y-Ling Liu, Mr. Shwe-Yi Chi, Ms. Choie-Wen Chou, Ms. Sy-Shin Lo and many assistants aided in the data preparation. Thanks are to Ms. Sy-Shin Lo for carrying out most of the computations and to Mr. Ching-Chi Wu for drafting some of the figures.

REFERENCES

CHEN, G. T. J., 1976: A composite case study of kinematic vertical motion. *Atmos. Sci.*, Meteor. Soc. Rep. of China, **3**, 87-105.

CHEN, G. T. J. and L. F. Bosart, 1977: Quasi-Lagrangian kinetic energy budgets of composite cyclone-anticyclone couplets. *J. Atmos. Sci.*, 34, 452-464.

GAMBO, K., 1970a: The characteristic feature of medium scale disturbances in the atmosphere (I). *J. Meteor. Soc. Japan*, **48**, 173-184.

GAMBO, K., 1970b: The characteristic feature of medium scale disturbances in the atmosphere (11). *Ibid*, **48** ,315-330.

HOLTON, J. R., 1972: *An Introduction to Dynamic Meteorology*. Academic Press, N. Y. and London, 319pp.

KUNG, E. C. and W. E. BAKER, 1975: Energy transformations in middle-latitude disturbances. *Quart. J. Roy. Meteor. Soc.* **101**, 793-815.

MATSUMOTO, S., S. YOSHIZUMI and M. TAKEUCHI, 1970: On the structure of the "Baiu front" and the associated intermediate scale disturbances in the lower atmosphere. *J. Meteor. Soc. Japan*, **48**, 479-491.

MATSUMOTO, S., K. NINOMIYA and S. YOSHIZUMI, 1971: Characteristic features of "Baiu" front associated with heavy rainfall. *Ibid*, **49**, 267-281.

NITTA, T. and J. YAMAMOTO, 1974: On the observational characteristics of intermediate scale disturbances generated near Japan and the vicinity. *Ibid*, **52**, 11-31.

O'BRIEN, J. J., 1970: Alternative solutions to the classical vertical velocity problem. *J. Appl. Meteor.*, **9**, 197-203.

RAMAGE, C. S., 1971: *Monsoon Meteorology*. Academic Press. N. Y. and London, 296pp.

TSAY, C. Y., 1975: Numerical weather prediction in the area of Taiwan and its vicinity. Dept. Atm. Sci., National Taiwan Univ., 43pp, (in Chinese with English abstract). NSC-64M-0202-01(11).

臺灣梅雨平均結構之個案研究

陳 泰 然
國立臺灣大學大氣科學系

摘 要

本文係針對臺灣梅雨季末期自一九七五年六月十日至十五日之六天資料進行分析研究，藉以瞭解梅雨區內天氣系統之平均結構及動能收支情況。由重力位高度、風、溫度、濕度、雲量及垂直運動等平均場之相互一致性得知原始資料主觀分析及所得結果之代表性及可靠性。並由平均垂直速度場得知在渦旋方程內之垂直傳送過程及扭轉效用在山區及斜壓區可能不容忽略。資料分析又顯示梅雨區內水氣之主要來源係遠自孟加拉灣。

由溫度場及垂直速度場得知，在梅雨區內盛行著暖空氣上升及冷空氣下降之熱力直接環流，這種環流在斜壓區，特別是在日本附近，顯得特別強烈。因此，平均動能收支之計算結果在梅雨區內有 $8.32\ W\ m^{-2}$ 之動能係導源於伴隨這種環流而來之跨越等高線氣流之過程所產生；而這些動能之增加亦在當地經由摩擦過程所消耗 ($-8.33\ W\ m^{-2}$)。梅雨區外經由跨越等高線過程轉換而有 $-5.55\ W\ m^{-2}$ 之動能消失，且於剩餘項內有 $4.91\ Wm^{-2}$ 之動能產生，此亦明顯指示梅雨區內外有著顯然不同的動力過程。